

Single crystal elasticity of gold (Au) up to ~20 GPa: Bulk modulus anomaly below ~5 GPa and implication for a primary pressure scale

*Akira Yoneda¹, Hiroshi Fukui², Gomi Hitoshi¹, Seiji Kamada⁴, Longjian Xie¹, Naohisa Hirao⁵, Hiroshi Uchiyama⁵, Satoshi Tsutsui⁵, Alfred Baron³

1. Institute for Planetary Materials, Okayama University, 2. Graduate School of Material Science, University of Hyogo, 3. Materials Dynamics Laboratory, RIKEN SPring-8 Center, 4. Graduate School of Science, Tohoku University, 5. Japan Synchrotron Radiation Research Institute

We measured single crystal elasticity of gold (Au) as well as its lattice parameters simultaneously under high pressure by using inelastic X ray scattering (IXS) technique. Generated pressure and elastic moduli of gold were obtained only from the present experimental data at five pressure points between 0 and 20 GPa by direct numerical integration. Pressure variation of the bulk modulus displays an anomalous behavior; it is nearly constant up to ~5 GPa, and then steeply increases toward higher pressure. Similar anomaly is observed in independent first-principles calculations as well. The absolute pressure scale determined from the present results gives systematically lower pressures than those from the previous pressure scales owing to the bulk modulus anomaly founded in this study.

Keywords: gold, single crystal elasticity, bulk modulus, pressure scale, inelastic X ray scattering, diamond anvil cell

High-pressure phase transitions of MgCO_3 under the lower mantle conditions

*Fumiya Maeda¹, Seiji Kamada², Tatsuya Sakamaki¹, Naohisa Hirao³, Yasuo Ohishi³, Akio Suzuki¹

1. Department of Earth Sciences, Graduate School of Science, Tohoku University, 2. Frontier Research Institute for Interdisciplinary Sciences, Tohoku University, 3. Japan Synchrotron Radiation Research Institute

MgCO_3 is one of the important carbonate minerals in the deep Earth because it can be a carbon carrier from the surface to the mantle in subduction processes. Such deep carbonates may be involved in melting of subducted rocks and formation of deep diamonds in the mantle transition zone or lower mantle. MgCO_3 has especially been suggested to be the most stable carbonate under the high-pressure and temperature conditions.

Recent experimental and theoretical studies reported high-pressure phase transitions of MgCO_3 under the lower mantle conditions. A report of the high-pressure polymorph was started from 'magnesite II' at 115 GPa in Isshiki et al. (2004). Several recent studies supported a monoclinic MgCO_3 ('phase II') as a post-magnesite phase above ~80 GPa.

Phase II was revealed to be composed of (C_3O_9) -ring units which were constituted by three CO_4 tetrahedra sharing three oxygen atoms. However, the structure of phase II has a little difference between the previous studies: the space groups of phase II were reported as C2/m and $\text{P2}_1/\text{c}$ in Oganov et al. (2008) and Boulard et al. (2011), respectively. Moreover the latest study by Pickard and Needs (2015) observed a new high-pressure polymorph having a triclinic lattice as a post-magnesite phase above 85 GPa, which changed to phase II at 101 GPa.

In addition to the difference of the post-magnesite phase and phase-II structures, none of the above studies decided the phase boundary of the high-pressure phase transitions at high temperature.

Therefore, we have been studied the phase relation of MgCO_3 up to the lowermost mantle conditions based on high-pressure and temperature experiments. We especially focused on the phase boundary of the high-pressure polymorphs at high temperature and a true post-magnesite phase.

The starting material was a natural magnesite from Bahia in Brazil. The experimental conditions were up to 138 GPa and 2900 K generated using a double-sided laser-heated diamond anvil cell (LHDAC). Culet diameters of diamond anvils used were between 130 and 250 μm . The sample was loaded into a sample chamber in a tungsten gasket which was pre-indented to 40–60 μm in thickness and drilled a 60–80- μm hole in diameter. Laser heating was conducted using a fiber laser. Pt or Au was used as a laser absorber. Run products were detected using synchrotron X-ray diffraction (XRD) measurements at beamline BL10XU of SPring-8 in Hyogo, Japan. Experimental pressures were measured using a thermal equation of state of Pt or Au (Fei et al., 2007) and thermal pressures were calculated using Mie-Grüneisen-Debye model (e.g., Fei et al., 1992). XRD patterns were analyzed using IPAnalyzer and PDIndexer software (Seto et al., 2010).

We observed the two high-pressure polymorphs of MgCO_3 , which might be monoclinic phase II and triclinic phase reported in Oganov et al. (2008) and Pickard and Needs (2015), respectively. Phase II was observed mainly above 90 GPa and the lattice constants were estimated to be $a = 8.209 \text{ \AA}$, $b = 6.575 \text{ \AA}$, $c = 6.978 \text{ \AA}$, $\beta = 104.06^\circ$, and $V = 365.3 \text{ \AA}^3$ at $100 \pm 2 \text{ GPa}$ and $2080 \pm 230 \text{ K}$ when fitted using the Oganov's space group, C2/m . The triclinic phase might be appeared as a post-magnesite phase around 90 GPa: The XRD patterns were not explained only by magnesite and phase II. Strong peaks near 104 diffraction of magnesite are considered to be derived from the triclinic phase although we could not fit their patterns and estimate the lattice constants due to lack of the peak number to fit the triclinic unit cell. We could estimate the phase boundaries of high-pressure polymorphs based on the above observations.

The triclinic post-magnesite phase may have a very narrow stability field in the P-T phase diagram. The triclinic phase might buffer the significant structural change from magnesite (CO_4 triangles) to phase II (C_3O_9 rings composed of three CO_4 tetrahedra).

Keywords: magnesite, high-pressure polymorph, lower mantle, LHDAC

What can mineral physics tell us about the origin of ULVZs?

*Catherine McCammon¹, Razvan Caracas²

1. Bayerisches Geoinstitut, University of Bayreuth, Germany, 2. Ecole Normale Supérieure de Lyon, France

The core-mantle boundary region is complex. In addition to large regions with reduced shear velocities (LLSVPs), there are small areas with shear velocities up to 30% lower than surrounding material, the so-called ultralow velocity zones (ULVZs). Although these heterogeneous regions are small (10 to 100 km), they have featured in speculation regarding an ancient global magma ocean, magnetic pole positions during reversals, core-mantle material exchange and the source of mantle plumes. Mineral physics provides important constraints in understanding the nature of ULVZs through the comparison of seismic data with experimental and computational studies of the relevant phases. Shear wave velocities are particularly important, and nuclear inelastic scattering (NIS) offers the attractive possibility to measure these velocities for iron-containing minerals in the laser-heated diamond anvil cell through direct measurement of the partial density of states (DOS). Complementary determination of the partial DOS using density functional theory (DFT) has shown the potential to identify experimental features that impact the velocity determination as demonstrated by our recent study on bridgmanite. We performed first-principles calculations to determine the iron partial DOS for $\text{Mg}_{0.75}\text{Fe}_{0.25}\text{SiO}_3$ post-perovskite. We calculated Debye sound velocities (which are closely related to the shear wave velocities) using the same approach as for experimental NIS data, and obtained velocities for $\text{Mg}_{0.75}\text{Fe}_{0.25}\text{SiO}_3$ post-perovskite that are consistent with literature values for MgSiO_3 and FeSiO_3 post-perovskite also calculated using DFT. In contrast, literature data on the Debye sound velocity determined experimentally using NIS is 35% lower than our calculated value, which led to previous suggestions that ULVZs originate from regions containing iron-rich post-perovskite. Our results show, however, that the lower NIS velocities in post-perovskite data likely arise from a similar artefact as the NIS bridgmanite data. The velocities derived from the DFT DOS of both bridgmanite and post-perovskite are consistent with seismic velocities of the bulk lower mantle, suggesting that ULVZs are likely not caused by iron-rich post-perovskite. Instead we favour previous suggestions that dense melts are a more plausible explanation.

Keywords: lower mantle, density functional theory, nuclear inelastic scattering, shear wave velocity, post-perovskite

Single crystal synthesis of δ -(Al,Fe)OOH using multi-anvil apparatus

*Itaru Ohira¹, Takaaki Kawazoe², Takayuki Ishii², Tiziana Boffa Ballaran², Catherine McCammon², Akio Suzuki¹, Eiji Ohtani^{1,3}

1. Department of Earth and Planetary Materials Science, Graduate School of Science, Tohoku University, 2. Bayerisches Geoinstitut, University of Bayreuth, 3. V.S. Sobolev Institute of Geology and Mineralogy, Siberian Branch, Russian Academy of Sciences

δ -AlOOH is an important hydrous mineral for understanding the water cycle in the deep Earth. In a descending slab, δ -AlOOH forms a solid solution with Phase H (MgSiO_4H_2) and ϵ -FeOOH [e.g., 1, 2]. This solid solution can transport water stored in its crystal structure to the deep mantle because it can be stable at the lowermost mantle conditions [1, 3]. Therefore, δ -AlOOH - Phase H - ϵ -FeOOH solid solution may affect the Earth's deep water cycles, chemical heterogeneity, and anomalies of seismic wave velocities at the lower mantle.

However, the stability, structure, elasticity, and spin state of this solid solution that are essential to discuss the issues above have not been constrained experimentally because of the difficulty to synthesize this solid solution as a homogeneous single phase.

In this study, we successfully synthesized Fe-bearing δ -AlOOH (δ -(Al, Fe)OOH) single crystals. Single crystals of pure δ -AlOOH and δ -(Al, Fe)OOH with dimensions up to ~ 0.6 mm were synthesized by a high-pressure hydrothermal method. Synthesis experiments were performed at 21 GPa and 1480 K for 4 h using a Kawai-type multianvil apparatus. Mössbauer spectra showed 95-100% $\text{Fe}^{3+}/\Sigma \text{Fe}$ at the octahedral site in δ -(Al, Fe)OOH. Unit-cell parameters of δ -AlOOH were consistent with those of previous studies, and they increased linearly with $\text{Fe}/(\text{Al}+\text{Fe})$ of the starting materials. The crystals contain 1-2 wt.% of excess water compared to their ideal water content. The syntheses of large single crystals of δ -(Al, Fe)OOH will facilitate investigations of their stability, elasticity, elastic anisotropy, spin state, and behavior of hydrogen bonding, which will improve our understanding of the water cycles, chemical heterogeneity, and anomalies of V_p and V_s in the deep Earth.

This work was supported by the JSPS Japanese-German Graduate Externship.

Reference

- [1] Ohira et al. (2014) *Earth and Planet. Sci. Lett.*, **401**, 12-17
- [2] Liu et al. (2016) *Goldschmidt Conference 2016*, **04d**, 10:45-11:00
- [3] Sano et al. (2008) *Geophys. Res. Lett.*, **35**, L03303

Keywords: Water Cycle in the Earth's Interior, High Pressure and High Temperature Experiment, δ -AlOOH, ϵ -FeOOH, Single Crystal, Kawai-type Multianvil Apparatus

Pressure-induced stacking disorder and non-symmetric hydrogen bond in boehmite

Yusuke Ishii¹, *Kazuki Komatsu¹, Satoshi Nakano², Shinichi Machida³, Takanori Hattori⁴, Asami Sano-Furukawa⁴, Hiroyuki Kagi¹

1. Geochemical Research Center, Graduate School of Science, The University of Tokyo, 2. National Institute for Materials Science, 3. Neutron Science and Technology Center, CROSS-Tokai, 4. J-PARC Center, JAEA

It has gradually been accepted that significant amount of 'water' can exist as hydrous minerals in the deep Earth, at least locally at subducting slab or mantle transition zone, from the observation of high-P and high-T experiments and diamond inclusions (e.g., Peacock (2000) *Science*, **248**, 329; Pearson *et al.* (2014) *Nature*, **507**, 221). Because the main rock-forming minerals in the deep Earth are oxide or silicate minerals, hydrogens in hydrous minerals are surrounded by oxygens, and they form O-H...O hydrogen bonds (H-bonds). At high pressure, H-bond symmetrization may occur owing to the shortening O...O distances, yielding the O-H and H...O distances are equivalent, so that H-bonds in hydrous minerals occurred under some depth could be symmetrized. However, there are only a few studies regarding the H-bond symmetrization in hydrous minerals (e.g., Tsuchiya *et al.* (2002) *Geophys Res Lett*, 29, 1; Sano-Furukawa *et al.* (2009) *Am Mineral*, **94**, 1255; Tsuchiya and Mookherjee (2015) *Sci Rep*, **5**, 15534), and little is known about the relation between H-bond symmetrization with compression and the physical property change. Here we show a structure variation of boehmite with increasing pressure observed by using in-situ x-ray/neutron diffraction methods and Raman spectroscopy under pressure, and first found that pressure-induced stacking disorder would prevent H-bond symmetrization.

Keywords: Boehmite, High Pressure, Stacking disorder

Dehydration kinetics of boehmite and diaspore

*Takaya Nagai¹, Kankichi Hattori², Jun Kawano¹, Ayako Shinozaki¹

1. Department of Earth & Planetary Sciences, Faculty of Science, Hokkaido University, 2. Division of Earth & Planetary Sciences, School of Science, Hokkaido University

Boehmite and diaspore are polymorphs of AlOOH . Dehydration kinetics of boehmite (H-boehmite), deuterated boehmite (D-boehmite) and diaspore were investigated by thermogravimetric measurements with various heating rates. During dehydration treatments, boehmite and diaspore convert to $\gamma\text{-Al}_2\text{O}_3$ and corundum, respectively. The extent of dehydration as a function of temperature and heating rate was analyzed by integral isoconversional methods proposed in Vyazovkin et al.(2011). Because obtained isoconversional activation energies vary significantly with conversion extent, dehydration processes of these hydrous minerals are dominated by not a single reaction but multiple reaction steps. Comparison between H-boehmite and D-boehmite suggests the early stage of dehydration process is controlled by hydrogen migration from one O-H group to adjacent O-H (formation of adsorbed water molecule). On the other hand, comparison between H-boehmite and diaspore suggests the latter stage of dehydration process is controlled by migration of the adsorbed water molecule.

Keywords: dehydration kinetics, boehmite, diaspore

Molecular Dynamics Study of Soret Effect in Calcium-Aluminosilicate glass

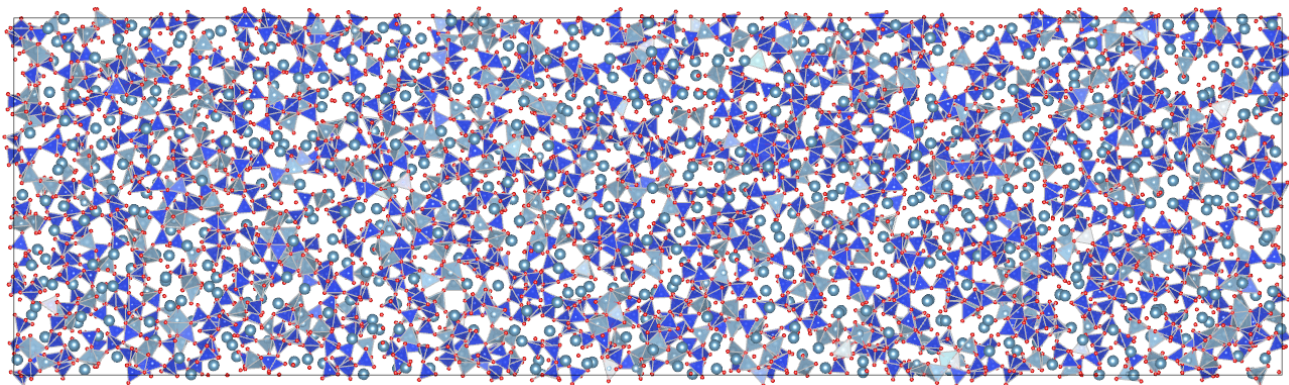
*Fumiya Noritake¹, Yukihiro Yoshida², Hirofumi Hidai³, Tetsuo Kishi², Nobuhiro Matsushita², Tetsuji Yano²

1. Graduate Faculty of interdisciplinary Research, University of Yamanashi, 2. Department of Materials Science and Engineering, Tokyo Institute of Technology, 3. Department of Mechanical Engineering, Chiba University

There are various transportation phenomena driven by a potential gradient. The Soret effect has been known as the diffusion driven by a temperature gradient (Soret, 1879; Ludwig, 1856). While the inverse one is known as Dufour effect. The Soret effect is sometime used in the explanation of fractionation phenomena in geology (Leshner, 1986; Dominguez et al., 2011). Recently Kishi et al. (2016, conference abstract) reports a distribution anomaly of composition around the trace of the migration of high-temperature metal sphere induced by laser irradiation in calcium aluminosilicate glass (Hidai et al., 2016). The rate of fractionation by temperature gradient is determined by both thermal diffusivity (D_T) and mass diffusivities (D) because the total net flux must be zero in a steady state. Consequently, understanding the Soret effect and determination of Soret coefficient (D_T/D) are difficult because the coefficient is affected by not only atomic mass and inter-atomic interaction that affect activation energy but also geometric/structural factor. Calcium-aluminosilicate system is suitable for the investigation of the Soret effect because three oxides have different characteristics; namely, network former, network modifier, and intermediate oxide.

We applied the molecular dynamics (MD) simulations for this system to investigate the mechanism of fractionation by temperature gradient. The MD simulation is an appropriate method for this study because it gives trajectories of each atoms in the simulation cells and potentials of each atom at any point in simulation time. MD simulations of $\text{Ca}_3\text{Al}_2\text{Si}_6\text{O}_{18}$ glass were performed using MXDORTO code (Sakuma & Kawamura, 2009). The simulation conditions are as follows: The inter-atomic potential model was taken from Noritake et al. (2015). System of approximately 30000 particles in rod-shaped (approximately $5 \times 5 \times 17$ nm) simulation cell in periodic boundary condition was firstly annealed for 2 ns at 1873 K from randomly generated structure. Then the liquid was quenched to room temperature at the rate of 10^{12} K/s. Then we started the simulations in temperature gradient. The temperatures in sliced regions (approximately 0.35 nm thickness) perpendicular to the longest axis at the end and the center of simulation cell were maintained 300 and 3500 K using the scaling procedure, respectively. After several tens nano-second simulations, we confirmed the changes in distribution of composition. The concentration of SiO_2 in the high-temperature center part slightly increases as simulation proceeds. In contrast the concentration of CaO in that part slightly decreases. The distribution of concentration of Al_2O_3 does not change apparently. Quantification of coefficient and mechanisms will be discussed in this presentation.

Keywords: Molecular Dynamics, Silicate Glass, Silicate Melt, Soret Effect



Phase transition of AlPO_4 -moganite: In-situ high-temperature Raman spectroscopic study

*Masami Kanzaki¹

1. Institute for Planetary Materials, Okayama University

Moganite-form of AlPO_4 has recently discovered as one of high-pressure phases (Kanzaki and Xue, 2012). Moganite is one of rare polymorphs of SiO_2 , and its structure is closely related to twinned quartz. For SiO_2 -moganite, temperature-induced displacive transition has been reported (Heaney et al., 2007). However, pure phase sample is difficult to obtain, and accordingly quality of data by Raman or diffraction is not good. Although AlPO_4 -moganite is easy to get pure phase, it is metastable at ambient pressure (moganite- SiO_2 is not stable phase either). In this study, phase transition in AlPO_4 -moganite was explored using in-situ high-temperature Raman spectroscopy up to 800 °C at ambient pressure. This transition was briefly mentioned in our 2011 this session talk, but completely new dataset, and additional low frequency data were obtained, and will be presented.

Used sample was same as that reported in our previous study (Kanzaki and Xue, 2012), and was synthesized at 5 GPa and 1500 °C. For heating, a wire heater was used (Kanzaki et al., 2012).

Temperature was calibrated using 5~6 substances with known melting points. For Raman measurement, a home-built confocal micro-Raman system was used (488 nm laser, ~80 mW, 500 mm polychromator, liquid N_2 cooled CCD detector). Initially, frequency region higher than 100 cm^{-1} was observed to 800 °C. Recently, our system is able to measure low frequency region, and two new peaks were identified at about 60 and 73 cm^{-1} at room temperature (see my talk last year). In order to check these peaks are soft mode or not, additional high-temperature study was conducted for < 100 cm^{-1} region. For the measurement, anti-Stokes and Stokes regions were observed simultaneously to identify true Raman peaks from the peaks originated from instrumental artifacts. The temperature is increased by 25 °C step, and increased up to 800 °C.

For the spectra measured above 100 cm^{-1} , several hard Raman modes displayed small shift to lower frequency with temperature. Above 425 °C, this trend was reversed or became nearly constant, and no discontinuity was observed. These results suggest that there is a displacive (higher order) phase transition at about 425 °C. For the region below 100 cm^{-1} , the 73 cm^{-1} peak showed significant temperature shift to lower frequency accompanied with significant broadening on the peak width. The peak disappeared at 475 °C. From these results, this peak is considered as soft mode. The 60 cm^{-1} peak shifted just like the hard mode noted above, and still remained above 475 °C. At around 800 °C, berlinite (stable phase) was observed.

Our study confirmed that AlPO_4 -moganite indeed has the displacive transition, and identified soft mode. For SiO_2 -moganite, only hard mode Raman was observed, and the transition temperature was determined as ~ 570 K (Heaney et al., 2007). No soft mode was reported to date. Our study suggests that soft mode for SiO_2 -moganite may exist at lower frequency region not studied yet. There is some differences in the transition temperature between obtained from hard mode and from soft mode. This is likely due to thermal non-equilibrium in the sample as heating rate was faster for latter (low frequency run). Further study including remeasurement and measurement at cooling process is in progress.

Heaney, P.J. et al. (2007) *Am. Mineral.*, 92, 631

Kanzaki, M. and Xue, X. (2012) *Inorg. Chem.*, 51, 6164

Kanzaki, M. et al. (2012) *J. Min. Petrol. Sci.*, 107, 114

Keywords: AlPO₄-moganite, soft mode, Raman spectroscopy

Symmetry reduction of analcime with Al/Si ordering

Neo Sugano¹, *Atsushi Kyono¹

1. Graduate School of Life and Environmental Sciences, University of Tsukuba

Analcime is a sodium aluminosilicate hydrate ($\text{NaAlSi}_2\text{O}_6 \cdot \text{H}_2\text{O}$) with the ANA type of zeolite framework. It occurs widely in hydrothermal and diagenetic environments. Symmetry of analcime is well known to be changed with distribution of framework cations and extra-framework cations. Naturally occurring analcime generally exhibits cubic symmetry space group $Ia\bar{3}d$, which is the maximum topological symmetry, but it can crystallize in at least three different symmetries; tetragonal space group $I4_1/acd$, orthorhombic space group $Ibca$, and monoclinic space group $I2/a$. However, crystallization conditions affecting the symmetry change have not been fully understood yet. In the study, we hydrothermally synthesized single crystals of analcime and hydrothermally re-heated under various heating time. Single crystals obtained from the different processes were refined by using single-crystal X-ray diffraction method.

Single crystals ranging in size from 50 to 120 μm were grown from gels of $\text{Al}_2(\text{SO}_4)_3$ and Na_2SiO_3 . They show deltoidal icositetrahedron habit with well-developed 24 equivalent $\{2\ 1\ 1\}$ crystal faces. Single crystals grown from gels possess cubic $Ia\bar{3}d$ symmetry, in which Si and Al are totally disordered over the framework T sites. Single crystals of analcime hydrothermally reheated for 24h, however, exhibit tetragonal $I4_1/acd$ symmetry. The tetragonal analcime shows a weak site preference of Si for $T1$ site and Al for $T2$ site. Single crystals of analcime hydrothermally reheated for 48h display orthorhombic $Ibca$ symmetry. In the orthorhombic analcime, Si and Al are strongly ordered over the T sites. Si is preferentially distributed into $T11$ and $T12$ sites whereas Al is into $T2$ site. The crystal structural analysis revealed continuous symmetry reduction from cubic $Ia\bar{3}d$ to orthorhombic $Ibca$ through tetragonal $I4_1/acd$ depending on heating time. On the other hand, Na atoms are equally distributed over the extra-framework sites during the symmetry reduction. The result of the study clearly shows the heating time significantly influences the Al/Si ordering over the framework T sites rather than the ordering of extra-framework cations. The symmetry reduction in analcime would be useful for understanding of petrological and geochemical history of rocks.

Keywords: analcime, single-crystal X-ray diffraction, Al/Si ordered distribution

Reexamination of the crystal structure of artinite, $\text{Mg}_2\text{CO}_3(\text{OH})_2 \cdot 3\text{H}_2\text{O}$, with two-dimensional disorder

*Gen-ichiro Yamamoto¹, Atsushi Kyono¹

1. Life and Environmental Sciences, University of Tsukuba

Artinite is a magnesium carbonate hydrate mineral with the formula $\text{Mg}_2\text{CO}_3(\text{OH})_2 \cdot 3\text{H}_2\text{O}$. It is known to possess a disordered structure in which carbonate groups and water molecules alternate statistically along *b*-axis (Akao and Iwai 1977). The Mg atoms are octahedrally coordinated by three hydroxyl groups, two water molecules, and one O(1) atom, and arranged in infinite chains parallel to *b*-axis by sharing edges. In the structure, half of the O(1) atoms is bounded to carbonate groups and the other half is to water molecules. It is therefore possible that in the disordered structure a carbonate group is arrayed at the next of a carbonate group along *b*-axis. However, if a carbonate group is positioned at the next of a carbonate group, the O-O distance between the carbonate groups is 0.894 Å, which is apparently shorter than the van der Waals radius of an O atom (1.40 Å). On the other hand, if the carbonate groups and water molecules strictly alternate along *b*-axis, a periodicity of two unit cell should appear along the *b*-axis. In the study, we reexamined the crystal structure of artinite and reconsidered the disordered configuration of carbonate group and water molecule in the structure.

Naturally occurring artinite (San Benito, USA) was used in the study. Single-crystal X-ray diffraction measurements were performed using Bruker APEXII ULTRA single-crystal diffractometer equipped with a CCD detector, multilayer optics, and graphite monochromated $\text{MoK}\alpha$ radiation ($\lambda = 0.71073$ Å) generated by a rotating anode. X-ray data were collected at a temperature of -173 °C using a N_2 -gas-flow cryostat. The crystal structure was solved by intrinsic phasing in the APEX2 software package and refined by full-matrix least squares using Shelxl-97 (Sheldrick, 1997). Computational chemistry calculations were performed using Gaussian 09 program (Frisch et al., 2009). Mulliken charges were calculated using Density Functional Theory (DFT) at B3LYP employing 6-31G basis set.

The refined cell parameters are $a = 16.468(8)$ Å, $b = 3.1352(15)$ Å, $c = 6.184(5)$ Å, $\beta = 98.702(5)^\circ$, space group $C2/m$. The unit cell corresponds to the totally disordered configuration of carbonate groups and water molecules on the *b*-lattice. The structure refinement converged to $R1 = 0.0339$, $wR2 = 0.0937$, and $\text{Goof} = 1.013$ for 414 reflections with $F_o > 4s(F_o)$. The bond distances in the MgO_6 octahedron are 2.0345(9) Å (2), 2.0610(13) Å, 2.1641(9) Å (2), and 2.0135(13) Å. Those in the carbonate group are 1.227(3) Å and 1.2920(18) Å (2). When the carbonate group is located at the next to the carbonate group along *b*-axis, the O-O distance between the neighboring O atoms in the carbonate groups is 0.8816(19) Å. The Mulliken charges of the neighboring O atom, O atom on the opposite side, and O atom bounded to Mg atom are -0.378, -0.721, and -0.845, respectively. That of C atom is 1.296.

Crystal structures of magnesium carbonate (hydrate) minerals are always composed of MgO_6 octahedra. Compared with the MgO_6 octahedra constituting hydromagnesite $\text{Mg}_5(\text{CO}_3)_4(\text{OH})_2 \cdot 4\text{H}_2\text{O}$, nesquehonite $\text{MgCO}_3 \cdot 3\text{H}_2\text{O}$, and magnesite MgCO_3 , the MgO_6 octahedron in artinite displays a large quadratic elongation parameter (Robinson et al. 1971). In addition, the carbonate group in artinite can be characterized by highly distorted geometry forming an acute isosceles triangle. The results of crystal structural analysis are in good agreement with those of previous research (Akao and Iwai, 1977).

Furthermore, our study completely supports the conclusion obtained in the early study that every chain running along *b*-axis has two possible positions of carbonate groups and water molecules, thus producing the two-dimensional disorder. The reason why the carbonate groups can be located at an unusual short distance would be explained by the strongly polarized charge distribution within the carbonate groups.

Keywords: Artinite, disordered configuration, single crystal structure analysis, ab initio calculation

Experimental investigation of the $\text{Fe}_2\text{O}_3\text{-As}_2\text{O}_5$ system in air

*Pierre Hudon¹, In-Ho Jung

1. McGill Univ.

Arsenic is notoriously harmful to the environment. In numerous deposits and mining concentrates, it is usually present in the form of sulfides such as arsenopyrite (FeAsS) and enargite (Cu_3AsS_4), arsenides such as loellingite (FeAs_2) and nickeline (NiAs), arsenates such as scorodite ($\text{FeAsO}_4 \cdot 2\text{H}_2\text{O}$), annabergite ($\text{Ni}_3(\text{AsO}_4)_2 \cdot 8\text{H}_2\text{O}$) and erythrite ($\text{Co}_3(\text{AsO}_4)_2 \cdot 8\text{H}_2\text{O}$) and solid solution in ore minerals such as chalcopyrite (CuFeS_2), pyrite (FeS_2), and sphalerite (Zn, FeS), for example. Currently, scorodite is the mineral of choice to immobilize arsenic from mine wastes because it has a very low solubility in water. Scorodite is also the most common arsenate known in nature where it is found in hydrothermal deposits and as a secondary mineral in gossans. Unfortunately, there is a lack of information in the literature regarding arsenate systems, which hamper the understanding of the complex chemical reactions involved in their genesis. In the last decades, much effort has thus been devoted to determine the thermodynamic properties and phase relations of arsenates in hydrous and anhydrous conditions. In this regard, the $\text{Fe}_2\text{O}_3\text{-As}_2\text{O}_5$ system is of particular interest because it contains the compound FeAsO_4 , the anhydrous analog of scorodite. Surprisingly though, the system $\text{Fe}_2\text{O}_3\text{-As}_2\text{O}_5$ is still poorly known. This is due to the hygroscopic nature, slow kinetics, and high volatility of its phases, and to the presence of iron, which prevent the use of platinum crucibles at high temperature. The first (and only) experimental investigation of the whole phase diagram was performed by Kasenov and Mustafin [*Russ. J. Inorg. Chem. (Engl. Transl.)*, 1997, 42, 1598-1599] using differential thermal analysis (DTA) and X-ray diffraction (XRD) up to 1100 °C. Unfortunately, experiments were performed in sealed but evacuated (to 10^{-6} bar, i.e. 10^{-3} mm Hg) silica crucibles and as a result, evaporation probably occurred during the runs. Moreover, the silica crucibles may have reacted with the starting materials, modifying the melting point of the solid phases and the oxidation state of both As and Fe in the system. Consequently, the experimental data collected by Kasenov and Mustafin (1997) may have produced a very different phase diagram than the one expected in air. To determine the correct $\text{Fe}_2\text{O}_3\text{-As}_2\text{O}_5$ phase diagram in air and minimize most of the problems cited above (hygroscopicity, slow kinetics, high volatility, and presence of Fe reacting with crucibles), we prepared dry starting materials, carried out long duration experiments (up to 36 days) with non-evacuated sealed $\text{Au}_{75}\text{Pd}_{25}$ crucibles up to 1000 °C using the quenching method and accomplished phase characterization using XRD, backscattered electron (BSE) imaging, and electron probe microanalysis (EPMA). Based on our experiments, new subsolidus phase relations are proposed for the $\text{Fe}_2\text{O}_3\text{-As}_2\text{O}_5$ phase diagram in air, which are significantly different from the ones published earlier by Kasenov and Mustafin (1997). We also report the existence of a new compound, $\text{Fe}_6\text{As}_4\text{O}_{19}$ (F_3A_2), which is a potential candidate for arsenic sequestration.

Keywords: Phase diagram, Iron arsenates, Scorodite, $\text{Fe}_6\text{As}_4\text{O}_{19}$

Quantitative determination of Al/Si-order parameter in sillimanite from micrometric region using HARECXS method

*Yohei Igami¹, Takahiro Kuribayashi², Akira Miyake¹

1. Graduate School of Science, Kyoto University, 2. Graduate School of Science, Tohoku University

Sillimanite is one of the polymorphs of Al_2SiO_5 which are valuable as indicators of pressure and temperature. Structure of sillimanite consists of AlO_6 octahedral chains and Si/AlO_4 tetrahedral double chains parallel to the *c*-axis. Although the tetrahedral Si/Al ions are normally ordered, a possibility of its disordering at high temperatures has been suggested (e.g. Zen, 1969). However, the Al/Si-order parameter of sillimanite has not been successfully quantified. The main problems are that one is the difficulty of separating mullite ($\text{Al}_2[\text{Al}_{2+2x}\text{Si}_{2-2x}]\text{O}_{10-x}$, $x \approx 0.17-0.59$) from sillimanite, because mullite is very similar to sillimanite crystallographically, and another is the difficulty to distinguish Al from Si using XRD experiments because of similarity of their X-ray scattering factor.

On the other hand, Atom location by channeling-enhanced microanalysis (ALCHEMI) using TEM-EDS was carried out for determination of Al/Si-order parameter in orthoclase by Taftø & Buseck (1983). By ALCHEMI, it can distinguish the elements with similar atomic number, e.g. Al and Si, and it can be quantified the Al/Si-order parameter from the only sillimanite micrometric region. Furthermore, HARECXS (High Angular Resolution Electron Channeling X-ray Spectroscopy), which was developed from ALCHEMI recently (e.g. Soeda, 2000; Yasuda *et al.*, 2006), provides more quantitative information, because of many EDS measurements by varying the direction of incident electron beam. In this study, therefore, HARECXS experiments were carried out on sillimanite to establish the determination procedure for the Al/Si-order parameter in sillimanite.

Sillimanite crystals in Rundvågshetta, East Antarctica, which are homogeneous without characteristic textures, were examined using TEM-EDS (JEOL JEM-2100F, JED-2300T). HARECXS profiles were obtained by collecting X-ray signals as a function of electron-beam direction. The Al/Si-order parameter was determined by comparison between the obtained HARECX profiles and simulated HARECXS profiles by program ICSC (Oxley & Allen, 2003). Additionally, CBED (convergent-beam electron diffraction) patterns were also obtained to estimate sample thickness. Moreover, single crystal X-ray diffraction experiment using an automated four-circle X-ray diffractometer (Rigaku, AFC-7S, Tohoku Univ.) with $\text{MoK}\alpha$ Radiation ($\lambda = 0.71069 \text{ \AA}$) was also carried out in order to evaluate the result obtained by HARECXS.

As the result, the HARECXS profiles were successfully obtained from $1.5 \mu\text{m}$ diameter region. For quantitative analysis, two types of profiles were simulated; a profile of ordered sillimanite and that of disordered sillimanite, using the sample thickness determined by CBED. The experimental profiles were successfully fitted to linear combination of the two simulated profiles, and Al/Si-order parameter was determined. The determined results of 18 measurements were converged around 0.80 regardless of sample thickness. However, single crystal XRD experiment showed the Al/Si-O bond distances corresponding to the Al/Si-order parameter of 0.88. The discrepancy are thought to be caused by estimation error of absorption coefficient of incident electron for sillimanite which is one of the simulation parameter to affect the HARECXS simulation. It suggests that the additional absorption should be required for more precise simulation.

The above analytical procedure was also successfully applied to experimentally heat-treated sillimanite, avoiding mullite or glasses formed by heat-treatment. Furthermore, the HARECXS method can also apply to various other minerals to determine site occupancies and estimate formation environment.

Keywords: ALCHEMI, HARECXS, sillimanite, order parameter, TEM